ACS Catalysis

Letter

pubs.acs.org/acscatalysis

The impact of Metal–Ligand Cooperation in Hydrogenation of Carbon Dioxide Catalyzed by Ruthenium PNP Pincer

Georgy A. Filonenko,[†,‡] Matthew P. Conley,[§] Christophe Copéret,[§] Martin Lutz,[⊥] Emiel J. M. Hensen,[†,‡] and Evgeny A. Pidko[†,‡,*]

[†]Inorganic Materials Chemistry, Department of Chemical Engineering, Eindhoven University of Technology, P.O. Box 513, 5600 MB Eindhoven, The Netherlands

[‡]Institute for Complex Molecular Systems, Eindhoven University of Technology, P.O. Box 513, 5600 MB Eindhoven, The Netherlands

[§]Department of Chemistry and Applied Biosciences, ETH Zürich, CH-8093 Zürich, Switzerland

[⊥]Crystal and Structural Chemistry, Bijvoet Center for Biomolecular Research, Utrecht University, Padualaan 8, 3584 CH Utrecht, The Netherlands

Supporting Information

ABSTRACT: The metal–ligand cooperative activation of CO_2 with pyridine-based ruthenium PNP pincer catalysts leads to pronounced inhibition of the activity in the catalytic CO_2 hydrogenation to formic acid. The addition of water restores catalytic performance by activating alternative reaction pathways and leads to unprecedented Ru-catalyzed CO_2 hydrogenation activity. The mechanism of the underlying chemical transformations is proposed on the basis of DFT calculations, kinetic experiments, and NMR reactivity studies.

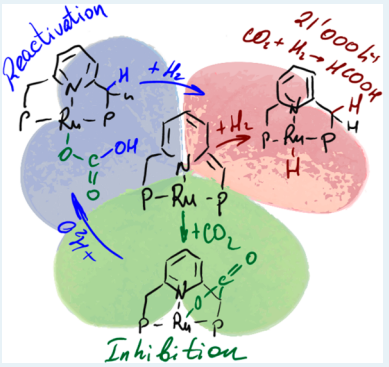

KEYWORDS: *metal–ligand cooperation, ruthenium, CO_2 hydrogenation, pincer catalyst*

The utilization of carbon dioxide as a C1 building block in chemical synthesis is gaining increasing attention and is driven by the necessity of sustainable chemical technologies.[1] Several pathways of CO_2 conversion have been proposed, such as CO_2 coupling with alkenes,[2a−c] alkynes,[2d] or epoxides,[3] to form functionalized products. Formation of methanol[4] or formic acid (FA) from CO_2 and renewable hydrogen paves the way toward the development of cleaner energy technologies.[5]

Recent efforts have shown that Fe complexes are promising catalysts for CO_2 hydrogenation,[6] yet the most efficient ones contain noble metals (i.e., Rh,[7b] Ir,[7c,8] Ru[7d,9]).[7a] For example, Nozaki and co-workers introduced the PNP pyridine-based pincer iridium trihydride that exhibits the highest reported turnover frequencies (TOF) of 150 000 h^{-1}.[8] They proposed that the PNP ligand is noninnocent and participates in CO_2 hydrogenation by assisting the metal center in heterolytic H_2 cleavage. The noninnocent behavior of nitrogen-centered pincer ligands is often invoked to explain the unique catalytic properties of this class of transition metal complexes.[10a] In the presence of a base, the pincer arm can undergo deprotonation, resulting in a five-coordinated species and an adjacent reactive site on the dearomatized ligand, as shown for the transformation of **1** → **2** in Scheme 1 for a related Ru derivative.[10] The unsaturated ruthenium complex **2** shows high reactivity toward addition of small molecules, such as CO_2 and H_2, to form **3**[11] and **4**,[12] respectively. The ligand-centered CO_2 activation, present in **3**, provides an intriguing intermediate for catalytic transformations of carbon dioxide. Ru-based pincer catalysts have attracted attention as hydrogenation catalysts for a wide range of polar substrates, including CO_2.[7d,9]

In this study, we combined catalytic activity measurements with in situ NMR spectroscopy and density functional theory (DFT) calculations to investigate the activity of **3** and **4** in CO_2 hydrogenation and to determine the role of different substrate activation modes in reactions catalyzed by noninnocent Ru–PNP complexes. In short, we report unprecedented ruthenium activity under mild conditions. We show that the cooperated activation of CO_2 in **3** to have a negative effect on catalysis, whereas water restores the activity by converting less active and stable intermediates into more catalytic competent ones.

As a starting point, we investigated catalytic CO_2 hydrogenation activity of complexes **3** and **4** (Figure 1a). Reactions were carried out at 70 °C in the presence of equimolar H_2/CO_2

Received: August 14, 2013
Revised: September 26, 2013
Published: October 4, 2013

   dx.doi.org/10.1021/cs4006869 | ACS Catal. 2013, 3, 2522–2526

Scheme 1. The Experimentally Observed Transformations of Ru-PNP Complexes in the Presence of H_2 and CO_2[a]

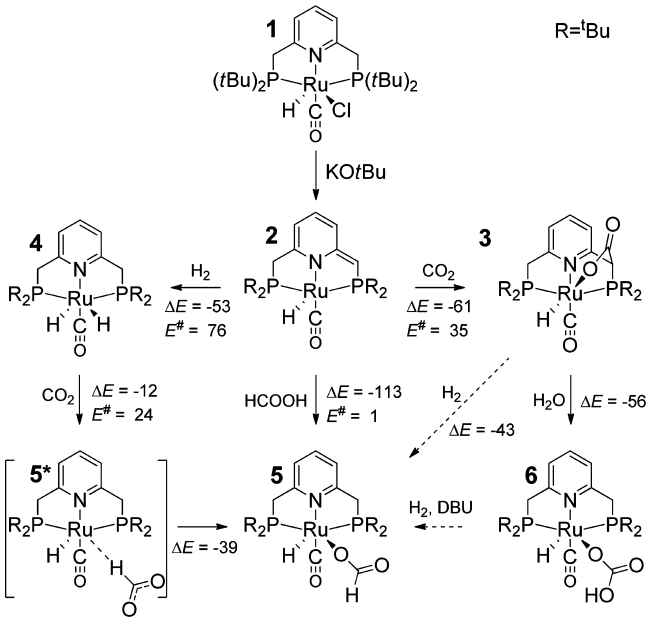

[a]5* is suggested by DFT. Solid arrows represent single-step reactions; dashed arrows correspond to the multistep transformations. The DFT-computed ZPE-corrected reaction (ΔE) and activation ($E^{\#}$) energies are given in kJ mol^{-1}.

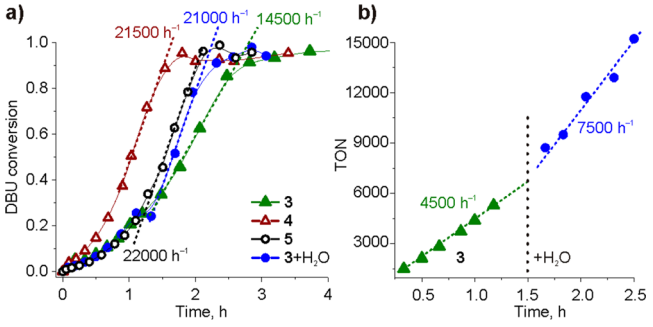

Figure 1. (a) Time-evolution of the formation of 2HCOOH·DBU adduct upon CO_2 hydrogenation (30/5 mL THF/DBU, $p(H_2/CO_2)$ = 40 bar, T = 70 °C) by complexes **3**, **4**, **5** (2.5 μmol), and **6** formed from **3** in the presence of H_2O. (b) The effect of H_2O injection on the catalytic reaction with **3** (0.53 μmol, $p(H_2/CO_2$ = 37/3) = 40 bar).

mixture (40 bar) in THF solutions containing DBU base (1,8-diazabicyclo[5.4.0]undec-7-ene) selected on the basis of the preliminary catalyst screening[13] and necessary to shift the reaction equilibrium toward formate formation.[14] Complex **3** gives high activity (TOF = 14 500 h^{-1}). An induction period is observed in this case, suggesting the transformation of **3** to the catalytically active state at the initial stage of the reaction. The combination of catalyst **4** and DBU allows reaching a TOF of 21 500 h^{-1} after a short induction period. In a separate experiment with lower catalyst concentrations, a TON of more than 90 000 was achieved with no catalyst deactivation observed (see Figure S1 in the Supporting Information). All catalytic runs resulted in a nearly quantitative conversion of DBU to the corresponding formate adduct (2HCOOH·DBU). To the best of our knowledge, we report the highest activity for Ru-based CO_2 hydrogenation system operating under non-supercritical conditions.[7,9]

We further combined in situ NMR spectroscopy supported by DFT calculations[15] to resolve the origin of the different behavior of catalysts **3** and **4**. Scheme 1 summarizes the chemical transformations evidenced by NMR and the respective DFT-computed reaction and activation energies. Complexes **3** and **4** are readily formed upon the ligand-assisted addition of CO_2 or H_2, respectively, to the dearomatized complex **2**.[11,12] The results of DFT calculations show that both reactions are thermodynamically favorable, although the formation of the dihydrido complex **4** is less exothermic and proceeds with a substantially higher activation barrier than the reaction with CO_2 to **3** (Scheme 1), suggesting that **3** may be present under catalytic conditions.

The ^{1}H NMR spectrum of **3** in THF-d_8 contains a low frequency ruthenium hydride resonance at −16.5 ppm as a doublet of doublets from coupling to two inequivalent phosphorus nuclei ($^2J_{PH}$ = 22 and 11 Hz). The ^{31}P NMR spectrum contains two signals at 115 and 109 ppm ($^2J_{PP}$ = 251 Hz). In the presence of H_2 or H_2/CO_2 mixtures, **3** is transformed to the Ru-formate complex **5** (Scheme 1). DFT shows that the reaction is strongly exothermic (ΔE = −43 kJ mol^{-1}). We speculate that this transformation proceeds via intermediate formation of **2** and **4** associated with substantial activation barriers. Related rearrangements of CO_2-added PNN-type pincer complexes were proposed to proceed via a similar deprotonated state.[11b] The ^{1}H NMR spectrum of **5** contains a new Ru−H signal at −16.5 ppm as a triplet ($^2J_{PH}$ = 20 Hz), and the ^{31}P NMR spectrum contains a broad singlet at 88 ppm, indicating that the phosphorus nuclei are equivalent. The ^{13}C NMR of **5** contains a signal at 170.9 ppm, which is consistent with formation of a metal formate complex. In the presence of hydrogen, **5** cannot be transformed back to **3**, and only partial (~16%, Supporting Information Figure S12) reversibility can be achieved under 3 bar CO_2 upon heating for 3 h. Thus, we propose that the formation of **3** under the reaction conditions is unlikely.

Experimentally, rapid formation of **5** is also observed upon the reaction of **4** and CO_2. The direct addition of CO_2 to the Ru−H moiety results in the computed metastable intermediate **5*** containing a noncoordinated $HCOO^-$ anion (ΔE = −12 kJ mol^{-1}, $E^{\#}$ = 24 kJ mol^{-1}), which rearranges to a more stable octahedral complex **5** (ΔE = −39 kJ mol^{-1}). Finally, **5** can be independently synthesized from benzene solutions of **2** contacted with FA vapors. DFT calculations predict that this reaction proceeds via barrierless protonation of the dearomatized PNP ligand in **2** (Scheme 1).

The solid-state structure of **5** is shown in Figure 2a. Complex **5** has an octahedral geometry and contains an η^1-coordinated formate moiety with a Ru1−O2 distance of 2.2457(13) Å, similar to that reported for other η^1-ruthenium formate complexes.[16] The ruthenium−ligand distances are nearly identical to a structurally related PNS−Ru formate complex, although the Ru−O bond is significantly longer in **5** than in the PNS−Ru formate (1.983 Å).[17]

The DFT results show a higher thermodynamic stability of **3** compared with **4**, which may account for its lower catalytic activity. Taken together with the results of the catalytic tests, this suggests that CO_2 hydrogenation is inhibited in the presence of **3** and that **4** could be one of the key intermediates of the catalytic cycle. To minimize the inhibiting effect of the ligand-assisted CO_2 activation and restore the catalytic activity, the decomposition of **3** has to be promoted.

dx.doi.org/10.1021/cs4006869 | ACS Catal. 2013, 3, 2522−2526

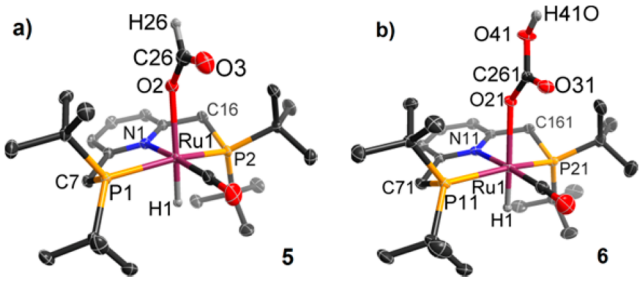

Figure 2. ORTEP diagrams of (a) **5** and (b) **6** plotted at 50% probability level. Hydrogen atoms of the PNP ligand and solvent molecules are omitted for clarity.[18] Selected distances and angles are discussed in the text. For details, refer to section 5 of the Supporting Information.

A plausible reaction path for the transformation of **3** to **4** in the presence of water was first identified by DFT calculations. A strongly exothermic hydrolysis of **3** (ΔE = −56 kJ mol^{-1}) results in the bicarbonate complex **6**.[19] The ligand-assisted decomposition of **6** to **2** in the presence of DBU is endoergic (ΔG°_{298K} > 0) and is not observed experimentally. Alternatively, **6** can undergo a hydrogenolysis reaction (Scheme 2).

Scheme 2. Proposed Mechanism of Hydrogenolysis of Formate and Carbonate Complexes 5 and 6, Respectively

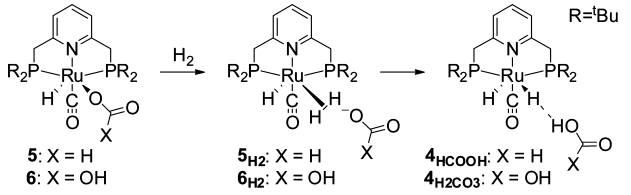

The HCO_3^- anion in **6** is substituted by H_2 to form $\mathbf{6}_{H_2}$ ($E^{\#}$ = 65 kJ mol^{-1}, ΔE = 31 kJ mol^{-1}). This step is followed by a facile heterolytic dissociation of H_2 ($E^{\#}$ = 6 kJ mol^{-1}, ΔE = −7 kJ mol^{-1}) to $\mathbf{4}_{H_2CO_3}$ (Scheme 2). Subsequent reaction with DBU is necessary to eliminate a DBU·H_2CO_3 adduct and to ensure the favorable thermodynamics for the overall process (**6** + H_2 + DBU → **4** + DBU·H_2CO_3, ΔE = −18 kJ mol^{-1}).

The hydrolysis of **3** can be experimentally observed. The NMR spectroscopic data are consistent with the predictions of DFT calculations. The ^{1}H NMR spectra of **3** in the presence of excess water (25−30 equiv of H_2O/Ru) showed a gradual decrease in the Ru−H resonance of **3** and the appearance of a new Ru−H resonance associated with **6**. The ^{1}H NMR spectrum of **6** contains a characteristic Ru−H signal as a triplet at −17.5 ($^2J_{PH}$ = 19 Hz) as well as a broad singlet at 85.8 ppm in the ^{31}P NMR spectrum. These resonances appear within minutes after addition of water to solutions of **3** in THF-d_8. The infrared spectrum of **6** contains a carbonate vibration at 1626 cm^{-1}. This value is close to the one obtained for another η^1-Ru bicarbonate complex.[20]

The solid-state structure of **6** is shown in Figure 2b. Compound **6** crystallizes as two polymorphs, triclinic and monoclinic, present in the same crystal (see section 5 in the Supporting Information). The structure of the major triclinic polymorph is presented in Figure 2b. The complex **6** is a distorted octahedron with P11−Ru1−P21 angle of 158.70(2)°. The ruthenium coordination sphere of **6** is nearly identical to that of **5**, and the ruthenium−oxygen bond distance is within 0.01 Å of the Ru−O bond in **5**. Complex **6** is a relatively rare example of a η^1-Ru-bicarbonate complex: most ruthenium bicarbonate complexes are η^2-coordinated.[21] Hydrolysis of **3** leads to nearly quantitative (93%) formation of **6** within an hour. This reaction can be applied at the stage of catalyst pretreatment to ensure the abundance of **6** in the reaction mixture.

Conversely, the addition of water has a pronounced beneficial effect on the catalytic activity of **3** in the hydrogenation of CO_2. Treatment of **3** with of ∼2000 equiv of H_2O/**3** prior to the catalytic test results in the activity similar to that observed for **4** (TOF = 21 000 h^{-1}), although the induction period is not avoided. The introduction of H_2O during the catalytic reaction in a low conversion experiment with **3** leads to a 50% increase in the hydrogenation rate (Figure 1b). The total conversion in this experiment was kept below 10% to ensure the accuracy of the performed test. These findings are consistent with the water-promoted transformation of **3** into a catalytically active state.

Further reactivity studies show that **6** can be transformed to **5** in the presence of H_2 and DBU. A possible mechanism would involve the reaction of **4** with DBU*H_2CO_3 that is the only carbon source available. Thus, the activity of the reactivated catalyst should resemble that of **5**.

Indeed, the catalytic behavior of **5** is identical to that of the **3**/H_2O system, that is, complex **6** (Figure 1a). DFT results point out that **5** is the most thermodynamically stable compound among the Ru-PNP derivatives considered here. This implies that **5** is a resting state rather than an intermediate in the catalytic cycle. Our proposition is supported by the fact that NMR experiments aimed at monitoring the catalytic reaction evidenced the sole formation of **5** (see Figure S10 in the Supporting Information).

DFT calculations can provide a molecular level insight into the mechanism of CO_2 hydrogenation over Ru-PNP catalyst (Figure 3). The catalytic cycle is initiated by the reaction of CO_2 and the Ru−PNP dihydride **4**, resulting in a transient

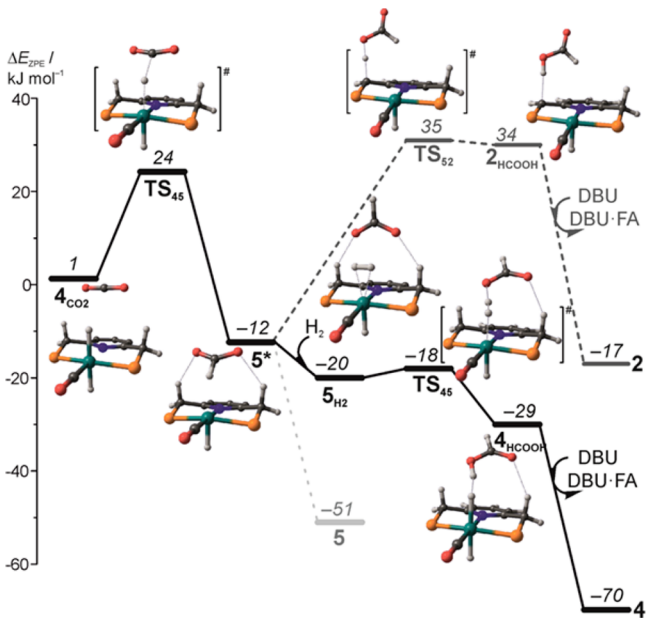

Figure 3. DFT-computed reaction energy diagram for CO_2 hydrogenation with **4**. Relative ZPE-corrected energies (italic) are given in kJ mol^{-1} with respect to **4**.

dx.doi.org/10.1021/cs4006869 | ACS Catal. 2013, 3, 2522−2526

intermediate **5***. The reaction can then proceed via three alternative channels. The direct coordinatation of the formate anion to the metal center gives **5**. Further transformations of **5** require the elimination of the $HCOO^-$ anion from the first coordination sphere of Ru. Alternatively, **5*** can be transformed via a ligand-assisted path involving an outer-sphere deprotonation of the PNP pincer arm by $HCOO^-$ (**5*** → $[\mathbf{TS}_{52}]^{\#}$ → $\mathbf{2}_{HCOOH}$, $E^{\#}$ = 47 kJ mol^{-1}; ΔE = 36 kJ mol^{-1}). A much more favorable pathway involves H_2 binding to the coordinatively unsaturated Ru center in **5*** (**5*** + H_2 → $\mathbf{5}_{H_2}$, ΔE = −8 kJ mol^{-1}), followed by heterolytic H_2 dissociation, resulting in $\mathbf{4}_{HCOOH}$ (Figure 3). This reaction is favorable and proceeds with a negligible activation barrier of 2 kJ mol^{-1} (Figure 3). Note that a similar reaction with the stable complex **5** (Scheme 2) is hampered by a high barrier ($E^{\#}$ = 65 kJ mol^{-1}) for the replacement of the coordinated formate anion with H_2 to yield $\mathbf{5}_{H_2}$. The catalytic cycle is closed by the reaction of $\mathbf{4}_{HCOOH}$ with DBU, resulting in the DBU·HCOOH product and the regeneration of the initial complex **4**.

These calculations allow us propose the origin of the prolonged induction period in catalysis with **5**. We believe that the abundance of this intermediate at the initial stage of the reaction is responsible for the lag time. Indeed, a maximal activity is expected when the steady state concentration of **5*** is reached. Although **4** is easily transformed to **5*** via CO_2 insertion, **5** meets a substantial barrier for related transformation. Thus, more time is required to build up **5*** from any other source, different from **4**.

In conclusion, we investigated the role of ligand-assisted transformations of pyridine-based Ru−PNP complexes in catalytic hydrogenation of CO_2. Although most reports highlight the beneficial role of ligand noninnocence, we found that pathways involving ligand participation are not contributing to the catalytic cycle. Moreover, **3**, the product of ligand-assisted CO_2 activation, is a rather inactive state that inhibits the catalytic performance. The addition of water converts **3** to **6** and restores the activity by providing a pathway toward formation of the active species. Formic acid is produced via an outer-sphere mechanism over **4**, in which a noncoordinated $HCOO^-$ anion, formed upon the initial CO_2 activation by Ru−H moiety, assists in the heterolytic dissociation of H_2. The stable Ru-formate complex **5** was identified as the resting state. It is demonstrated that Ru−PNP catalyst in combination with DBU is exceptionally active under mild conditions. The results presented here provide new insight into the subtle mechanistic pathways that can be encountered in CO_2 hydrogenation.

■ ASSOCIATED CONTENT

Supporting Information

Experimental and computational details; supplementary catalytic, NMR, and XRD experimental results; optimized structures of all intermediatae and transition states; computed reaction and activation Gibbs free energies. This material is available free of charge via the Internet at http://pubs.acs.org.

■ AUTHOR INFORMATION

Corresponding Author

*E-mail: e.a.pidko@tue.nl.

Notes

The authors declare no competing financial interest.

■ ACKNOWLEDGMENTS

E.A.P. thanks the Technology Foundation STW and The Netherlands Organization for Scientific Research (NWO) for his personal VENI Grant. Supercomputer facilities were provided by SurfSARA and NWO. The X-ray diffractometer has been financed by NWO.

■ REFERENCES

(1) (a) Cokoja, M.; Bruckmeier, C.; Rieger, B.; Herrmann, W. A.; Kühn, F. E. *Angew. Chem., Int. Ed.* **2011**, *50*, 8510. (b) *Carbon dioxide as chemical feedstock*; Aresta, M., Ed.; Wiley-VCH: Weinheim, 2010. (c) Sakakura, T.; Choi, J.-C.; Yasuda, H. *Chem. Rev.* **2007**, *107*, 2365. (d) Huang, K.; Sun, C.-L.; Shi, Z.-J. *Chem. Soc. Rev.* **2011**, *40*, 2435.

(2) (a) Greenhalgh, M. D.; Thomas, S. P. *J. Am. Chem. Soc.* **2012**, *135*, 11900. (b) Ohishi, T.; Zhang, L.; Nishiura, M.; Hou, Z. *Angew. Chem., Int. Ed.* **2011**, *35*, 8114. (c) Lejkowski, M. L.; Lindner, R.; Kageyama, T.; Bódizs, G. É.; Plessow, P. N.; Müller, I. B.; Schäfer, A.; Rominger, F.; Hofmann, P.; Futter, C.; Schunk, S. A.; Limbach, M. *Chem.—Eur. J.* **2012**, *18*, 14017. (d) Zhang, L.; Cheng, J.; Carry, B.; Hou, Z. *J. Am. Chem. Soc.* **2012**, *134*, 14314.

(3) (a) Whiteoak, C. J.; Kielland, N.; Laserna, V.; Escudero-Adan, E. C.; Martin, E.; Kleij, A. *J. Am. Chem. Soc.* **2013**, *135*, 1228. (b) Chatelet, B.; Joucla, L.; Dutasta, J.-P.; Martinez, A.; Szeto, K. C.; Dufaud, V. *J. Am. Chem. Soc.* **2013**, *135*, 5348. (c) Sakai, T.; Tsutsumi, Y.; Ema, T. *Green Chem.* **2008**, *10*, 337.

(4) (a) Olah, G. *Angew. Chem., Int. Ed.* **2005**, *44*, 2636. (b) Olah, G.; Surya Prakash, G. K.; Goeppert, A. *J. Am. Chem. Soc.* **2011**, *133*, 12881. (c) Hölscher, M.; Gürtler, C.; Keim, W.; Müller, T. E.; Peters, M.; Leitner, W. *Z. Naturforsch.* **2012**, *67b*, 961.

(5) (a) Boddien, A.; Mellmann, D.; Gärther, F.; Jackstell, R.; Junge, H.; Dyson, P.; Laurenczy, G.; Ludwig, R.; Beller, M. *Science* **2011**, *333*, 1733. (b) Fellay, C.; Dyson, P. J.; Laurenczy, G. *Angew. Chem., Int. Ed.* **2008**, *47*, 3966. (c) Boddien, A.; Federsel, C.; Sponholz, P.; Mellmann, D.; Jackstell, R.; Junge, H.; Laurenczy, G.; Beller, M. *Energy Environ. Sci.* **2012**, *5*, 8907. (d) Joó, F. *ChemSusChem.* **2008**, *1*, 805.

(6) (a) Ziebart, C.; Federsel, C.; Anbarasan, P.; Jackstell, R.; Baumann, W.; Spannenberg, A.; Beller, M. *J. Am. Chem. Soc.* **2012**, *134*, 20701. (b) Langer, R.; Diskin-Posner, Y.; Leitus, G.; Shimon, L. J. W.; Ben-David, Y.; Milstein, D. *Angew. Chem., Int. Ed.* **2011**, *50*, 9948. (c) Federsel, C.; Boddien, A.; Jackstell, R.; Jennerjahn, R.; Dyson, P. J.; Scopelliti, R.; Laurenczy, G.; Beller, M. *Angew. Chem., Int. Ed.* **2010**, *49*, 9777.

(7) (a) Federsel, C.; Jackstell, R.; Beller, M. *Angew. Chem., Int. Ed.* **2010**, *49*, 6254. (b) Angermund, K.; Baumann, W.; Dinjus, E.; Fornika, R.; Görls, H.; Kessler, M.; Krüger, C.; Leitner, W.; Lutz, F. *Chem.—Eur. J.* **1997**, *3*, 755. (c) Himeda, Y.; Onozawa-Komatsuzaki, N.; Sugihara, H.; Kasuga, K. *Organometallics* **2007**, *26*, 702. (d) Jessop, P. G.; Hsiao, Y.; Ikariya, T.; Noyori, R. *J. Am. Chem. Soc.* **1996**, *118*, 344.

(8) Tanaka, R.; Yamashita, M.; Nozaki, K. *J. Am. Chem. Soc.* **2009**, *131*, 14168. Tanaka, R.; Yamashita, M.; Chung, L. W.; Morokuma, K.; Nozaki, K. *Organometallics* **2011**, *30*, 6742.

(9) (a) Munshi, P.; Main, A. D.; Linehan, J. C.; Tai, C.-C.; Jessop, P. G. *J. Am. Chem. Soc.* **2002**, *124*, 7963. For more recent examples on the reactivity of Ru complexes, see: (b) Urakawa, A.; Jutz, F.; Laurenczy, G.; Baiker, A. *Chem.—Eur. J.* **2007**, *13*, 3886. (c) Huff, C. A.; Sanford, M. S. *J. Am. Chem. Soc.* **2011**, *133*, 18122. (d) Dub, P. A.; Ikariya, T. *ACS Catal.* **2012**, *2*, 1718.

(10) Reactivity and noninnocent behavior of pincer ligands: (a) Gunanathan, C.; Milstein, D. *Acc. Chem. Res.* **2011**, *44*, 588. (b) Benito-Garagorri, D.; Kirchner, K. *Acc. Chem. Res.* **2008**, *41*, 201. (c) Van der Vlugt, J. I.; Reek, J. N. H. *Angew. Chem., Int. Ed.* **2009**, *48*, 8832. (d) Balaraman, E.; Gunanathan, C.; Zhang, J.; Shimon, L. J.; Milstein, D. *Nat. Chem.* **2011**, *3*, 609. (e) Friedrich, A.; Drees, M.; Käss, M.; Herdtweck, E.; Schneider, S. *Inorg. Chem.* **2010**, *49*, 5482. (f) For a computational study, see: Yang, X. *ACS Catal.* **2011**, *1*, 849.

(11) (a) Vogt, M.; Gargir, M.; Iron, M. A.; Diskin-Posner, Y.; Ben-David, Y.; Milstein, D. *Chem.—Eur. J.* **2012**, *18*, 9194. (b) Huff, C. A.; Kampf, J. W.; Sanford, M. S. *Organometallics* **2012**, *31*, 4643.
(12) Examples of related dihydrido PNP and PNN pincer complexes: (a) Zhang, J.; Leitus, G.; Ben-David, Y.; Milstein, D. *J. Am. Chem. Soc.* **2005**, *127*, 10840. (b) Khaskin, E.; Iron, M. A.; Shimon, L. J. W.; Zhang, J.; Milstein, D. *J. Am. Chem. Soc.* **2010**, *132*, 8542.
(13) DBU was chosen on the basis of the results of the preliminary small-scale catalytic batch experiments with **1**. For comparison, under the same conditions, Et_3N gives TON = 750 (EtOH) and 160 (THF) when DBU/THF gave TON = 1960 (see Supporting Information for details).
(14) (a) Schaub, T.; Paciello, R. A. *Angew. Chem., Int. Ed.* **2011**, *50*, 7278. (b) Zhang, Z.; Hu, S.; Song, J.; Li, W.; Yang, G.; Han, B. *ChemSusChem* **2009**, *2*, 234.
(15) The calculations were performed using the Gaussian 09 program[22] with the PBE0 exchange-correlation functional and 6-311G(d,p) basis set for all atoms except ruthenium, which was described using a LanL2DZ basis set. The polarizable continuum model (PCM) was used to approximate the medium. All complexes were treated as neutral species. The accuracy of this method was tested by performing single-point calculations on selected reaction paths using a larger 6-311+G(d,p) basis set for all light atoms and TZVPP for Ru. The deviation in computed reaction energy did not exceed 2 kJ/mol. See the Supporting Information for the discussion of the selected methodology .
(16) (a) Barrata, W.; Ballico, M.; Del Zotto, A.; Herdtweck, E.; Magnolia, S.; Peloso, R.; Siega, K.; Toniutti, M.; Zangrando, E.; Rigo, P. *Organometallics* **2009**, *28*, 4421. (b) Bontemps, S.; Vendier, L.; Sabo-Etienne, S. *Angew. Chem., Int. Ed.* **2012**, *51*, 1671.
(17) Gargir, M.; Ben-David, Y.; Leitus, G.; Diskin-Posner, Y.; Shimon, L. J. W.; Milstein, D. *Organometallics* **2012**, *31*, 6207.
(18) CCDC 948170-948172 contain the supplementary crystallographic data for this paper. These data can be obtained free of charge from The Cambridge Crystallographic Data Centre via www.ccdc.cam.ac.uk/data_request/cif.
(19) Unfortunately, we were not able to identify a transition state for this path by DFT calculations. A related transformation was described for H_2O-assisted cleavage of C−C bonds during the decarboxylation of mandelylthiamine: Howe, G. W.; Bielecki, M.; Kluger, R. *J. Am. Chem. Soc.* **2012**, *134*, 20621.
(20) Jazzar, R. F.; Bhatia, P. H.; Mahon, M. F.; Whittlesey, M. K. *Organometallics* **2003**, *22*, 670.
(21) (a) Ellul, C. E.; Saker, O.; Mahon, M. F.; Apperley, D. C.; Whittlesey, M. K. *Organometallics* **2008**, *27*, 100. (b) Allen, O. R.; Dalgarno, S. J.; Field, L. D.; Jensen, P.; Willis, A., C. *Organometallics* **2009**, *28*, 2385.
(22) Frisch, M. J.; Trucks, G. W.; Schlegel, H. B.; Scuseria, G. E.; Robb, M. A.; Cheeseman, J. R.; Scalmani, G.; Barone, V.; Mennucci, B.; Petersson, G. A.; Nakatsuji, H.; Caricato, M.; Li, X.; Hratchian, H. P.; Izmaylov, A. F.; Bloino, J.; Zheng, G.; Sonnenberg, J. L.; Hada, M.; Ehara, M.; Toyota, K.; Fukuda, R.; Hasegawa, J.; Ishida, M.; Nakajima, T.; Honda, Y.; Kitao, O.; Nakai, H.; Vreven, T.; Montgomery, J. A., Jr.; Peralta, J. E.; Ogliaro, F.; Bearpark, M.; Heyd, J. J.; Brothers, E.; Kudin, K. N.; Staroverov, V. N.; Kobayashi, R.; Normand, J.; Raghavachari, K.; Rendell, A.; Burant, J. C.; Iyengar, S. S.; Tomasi, J.; Cossi, M.; Rega, N.; Millam, N. J.; Klene, M.; Knox, J. E.; Cross, J. B.; Bakken, V.; Adamo, C.; Jaramillo, J.; Gomperts, R.; Stratmann, R. E.; Yazyev, O.; Austin, A. J.; Cammi, R.; Pomelli, C.; Ochterski, J. W.; Martin, R. L.; Morokuma, K.; Zakrzewski, V. G.; Voth, G. A.; Salvador, P.; Dannenberg, J. J.; Dapprich, S.; Daniels, A. D.; Farkas, Ö.; Foresman, J. B.; Ortiz, J. V.; Cioslowski, J.; Fox, D. J. *Gaussian 09, Revision D.01*; Gaussian, Inc.: Wallingford, CT, 2009.